



**EUROfusion**

EUROFUSION WPMST1-PR(16) 15319

FM Laggner et al.

**Inter-ELM pedestal evolution: High  
frequency magnetic fluctuations  
correlated with the clamping of the  
pressure gradient**

Preprint of Paper to be submitted for publication in  
43rd European Physical Society Conference on Plasma  
Physics (EPS)



This work has been carried out within the framework of the EUROfusion Consortium and has received funding from the Euratom research and training programme 2014-2018 under grant agreement No 633053. The views and opinions expressed herein do not necessarily reflect those of the European Commission.

This document is intended for publication in the open literature. It is made available on the clear understanding that it may not be further circulated and extracts or references may not be published prior to publication of the original when applicable, or without the consent of the Publications Officer, EUROfusion Programme Management Unit, Culham Science Centre, Abingdon, Oxon, OX14 3DB, UK or e-mail [Publications.Officer@euro-fusion.org](mailto:Publications.Officer@euro-fusion.org)

Enquiries about Copyright and reproduction should be addressed to the Publications Officer, EUROfusion Programme Management Unit, Culham Science Centre, Abingdon, Oxon, OX14 3DB, UK or e-mail [Publications.Officer@euro-fusion.org](mailto:Publications.Officer@euro-fusion.org)

The contents of this preprint and all other EUROfusion Preprints, Reports and Conference Papers are available to view online free at <http://www.euro-fusionscipub.org>. This site has full search facilities and e-mail alert options. In the JET specific papers the diagrams contained within the PDFs on this site are hyperlinked

# Inter-ELM pedestal evolution: High frequency magnetic fluctuations correlated with the clamping of the pressure gradient

F. M. Laggner<sup>1</sup>, E. Wolfrum<sup>2</sup>, F. Mink<sup>2,3</sup>, M. Cavedon<sup>2,3</sup>, M. G. Dunne<sup>2</sup>, P. Manz<sup>2,3</sup>,  
G. Birkenmeier<sup>2,3</sup>, R. Fischer<sup>2</sup>, M. Maraschek<sup>2</sup>, E. Viezzer<sup>2</sup>, M. Willensdorfer<sup>2</sup>,  
F. Aumayr<sup>1</sup>, the EUROfusion MST1 Team\* and the ASDEX Upgrade Team<sup>2</sup>

<sup>1</sup> *Institute of Applied Physics, TU Wien, Fusion@ÖAW, 1040 Vienna, Austria*

<sup>2</sup> *Max Planck Institute for Plasma Physics, 85748 Garching, Germany*

<sup>3</sup> *Physik-Department E28, Technische Universität München, 85748 Garching, Germany*

\* See <http://www.euro-fusionscipub.org/mst1>.

The widely accepted theory to explain the stability limit of the pedestal is the peeling-ballooning theory [1]. However, the temporal approach of this limit, i.e. the inter-ELM profile evolution, is still not fully understood. The evolution of the inter-ELM electron density ( $n_e$ ) and electron temperature ( $T_e$ ) profiles has been the subject of detailed investigations, utilising fast edge profile measurements [2]. It has been found that the fully developed maximum gradients of density and temperature prior to the ELM onset stay almost constant for a period of the order of milliseconds. In this last phase of the ELM cycle, several experiments [3, 4, 5, 6] report the onset of high frequency magnetic fluctuations with frequencies larger than 150 kHz that originate from the plasma edge region.

This contribution analyses the magnetic fluctuations in detail, giving a deeper insight in the structure of the underlying instability and its propagation. Furthermore, linear magnetohydrodynamic (MHD) stability analyses were performed, for the phases, when the high frequency magnetic fluctuations are present.

In the following, two exemplary discharges with different pedestal top collisionalities ( $\nu_{e,\text{ped}}^*$ ) and similar electron pressure ( $p_e$ ) profiles are presented. These were conducted at a plasma current of 1 MA,  $-2.5$  T toroidal magnetic field (negative sign stands for opposite direction to the plasma current) in lower single null configuration and with similar plasma shape. The variation of collisionality simultaneously keeping fixed the pressure pedestal was achieved by a variation of heating power and externally applied gas puff. The ELM frequency in the low collisionality case ( $\nu_{e,\text{ped}}^* \approx 0.6$ , #30721) is larger than in the high collisionality case ( $\nu_{e,\text{ped}}^* \approx 1.5$ , #30701) since the heating power is higher. In both discharges a clamping of the pedestal pressure gradients before the ELM is correlated with the onset of radial magnetic fluctuations ( $\partial B_r/\partial t$ ) with frequencies above 200 kHz. Figure 1 presents an ELM-synchronised spectrogram of  $\partial B_r/\partial t$  in the top plot and ELM-synchronised time traces of the maximum electron density gradient ( $\max(-\nabla n_e)$ , blue), the maximum electron temperature gradient ( $\max(-\nabla T_e)$ , red) and inner divertor current (black). Although the ELM frequency varies slightly in the analysed interval, the pedestal recovery is very similar for each ELM until the pre-ELM temperature gradient (directly related to the pre-ELM pressure gradient) is reached. This can be seen in the evolution of the ( $\max(-\nabla n_e)$ , blue) and the maximum electron temperature gradient ( $\max(-\nabla T_e)$ ,

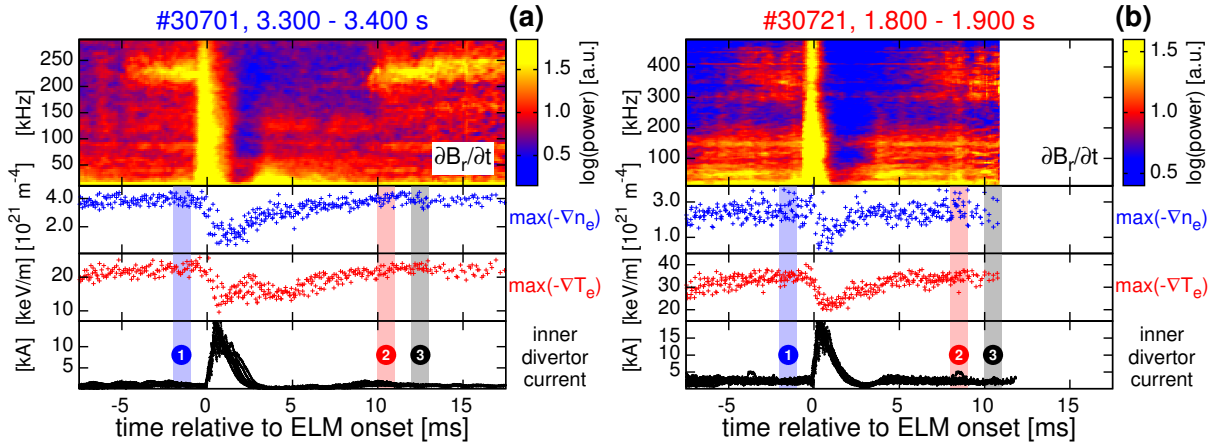


Figure 1: Pedestal evolution for high ((a), #30701) and low collisionality ((b), #30721): ELM-synchronised spectrogram of  $\partial B_t/\partial t$  and ELM-synchronised time traces of  $\max(-\nabla n_e)$  (blue),  $\max(-\nabla T_e)$  (red) and inner divertor current (black). The vertical bars and numbers indicate the phases in which the linear MHD stability analyses were performed. In both discharges, after  $\max(-\nabla T_e)$  is recovered (10 ms (#30701) respectively 8 ms (#30721) after the ELM onset) fluctuations set in. Figures modified from [6].

red). First, the  $\max(-\nabla n_e)$  is re-established (approximately 4 ms after the ELM onset), then the  $\max(-\nabla T_e)$  recovers. Correlated to the recovery of  $\max(-\nabla n_e)$  the onset of magnetic fluctuations in the region of up to 150 kHz is observed (4 ms after the ELM onset). These fluctuations are then present throughout the ELM cycle and related to low toroidal mode numbers ( $n$ ). When the  $\max(-\nabla T_e)$  is re-established (10 ms after the ELM onset) magnetic fluctuations with rather high frequencies 240 kHz (#30701) and 375 kHz (#30721) start. These fluctuations continue till the next ELM crash. Only marginal changes in  $\max(-\nabla n_e)$  and  $\max(-\nabla T_e)$  can be seen during this period. The next ELM crash interrupts the fluctuations, which set in again after the recovery of  $\max(-\nabla n_e)$  and  $\max(-\nabla T_e)$ . The onset of the high frequency fluctuations is clearly correlated with the recovery of the  $T_e$  pedestal and, consequently, the  $p_e$  pedestal (since the  $n_e$  pedestal recovers before). This observation can be explained by a saturated mode that sets in when a certain threshold (in terms of pedestal gradients) is reached. The mode is then affected either by the ELM crash itself, or the ELM-induced flattening of the pedestal leads to the vanishing of the drive. It has been observed that the high frequency fluctuations sometimes disappear shortly before the ELM onset ( $< 0.5$  ms), which then could be related to a possible ELM trigger mechanism [7].

The detected fluctuation frequency strongly differs for the presented cases, nevertheless, the onset of the high frequency fluctuations is strongly correlated with the pedestal pressure (temperature) recovery. This robust mechanism has been observed for a variety of plasma discharges. Several discharges performed with the same plasma current (1 MA) and toroidal magnetic field (-2.5 T) are analysed, to investigate the origin and structure of the high frequency fluctuations. An explanation for the detected fluctuation frequency is the strong background ( $E \times B$ ) flow, present in the pedestal region, mainly caused by the radial electric field. In H-mode, the flows

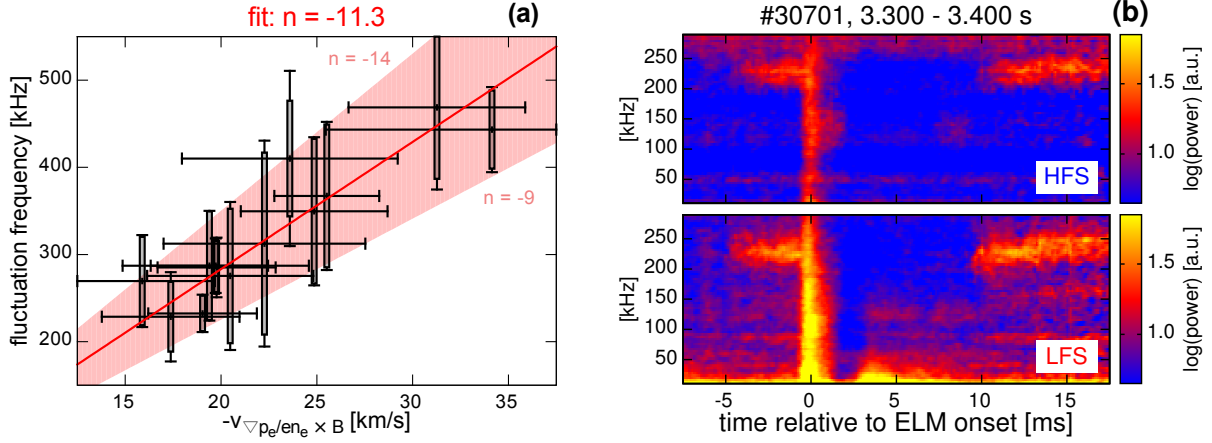


Figure 2: Neoclassically estimated background velocity and comparison of LFS and HFS fluctuations: (a) fluctuation frequency over  $-v_{\nabla p_e / e n_e}$  ( $\propto v_{E \times B}$ ). From the linear dependence between the detected fluctuation frequency and the background flow velocity a toroidal mode number  $n$  of approximately -11 can be determined (red line). (b) Spectrogram of the HFS (top) and the LFS ballooning coil signals. The high frequency fluctuations are also detected on the HFS. Figure modified from [6].

at the plasma edge can be described by neoclassical theory. At low toroidal rotation the term  $\nabla p_i / e n_i$  (using the main ion pressure ( $p_i$ ) and main ion density ( $n_i$ )) is the dominant contribution to the radial electric field. Here, this term is approximated by  $\nabla p_e / e n_e$  to give a proxy for the  $E \times B$  background velocity. Figure 2a presents the fluctuation frequency (considering only frequency bands at a statistical distribution  $> 200$  kHz) with respect to  $v_{\nabla p_e / e n_e} \times B$ , taken at the position of the maximum electron pressure gradient ( $\max(-\nabla p_e)$ , averaged between  $-2.0$  and  $-0.5$  ms relative to the ELM onset). A linear dependence between fluctuation frequency and  $-v_{\nabla p_e / e n_e}$  is observed, suggesting that the average detected frequency (in the lab frame) is caused by the background  $E \times B$  flow at the edge. Assuming similar mode structures for all analysed discharge intervals, a linear fit (red line) gives the toroidal ( $n$ ) and poloidal ( $m$ ) mode numbers. Using the safety factor ( $q$ ), the poloidal and toroidal plasma circumference leads to  $m \approx -55$  and corresponding  $n \approx -11$  (with  $q \approx 5$ ; negative sign corresponds to counter-current or electron diamagnetic direction). These numbers agree well with the mode numbers that can be determined from toroidally distributed magnetic pickup coils [6].

Deeper insight in the poloidal structure of the high frequency fluctuations gives the comparison of LFS and high field side (HFS) magnetic measurements. The comparison of ELM-synchronised spectrograms of  $\partial B_r / \partial t$  (figure 2b) from LFS and HFS shows that the high frequency fluctuations are also present on the HFS at similar frequency and phases relative to the ELM onset. This points in the direction of a mode with significant amplitude on the HFS, which is not expected for ballooning modes.

To investigate the linear MHD stability and possible drives for instabilities, linear MHD stability analyses were performed for the discharges presented in figure 1 (#30701, #30721). The utilised stability chain, using pressure constrained equilibrium data from IDE [8], the HELENA equilibrium code and a fast version of the MHD code MISHKA, is described in reference [9].

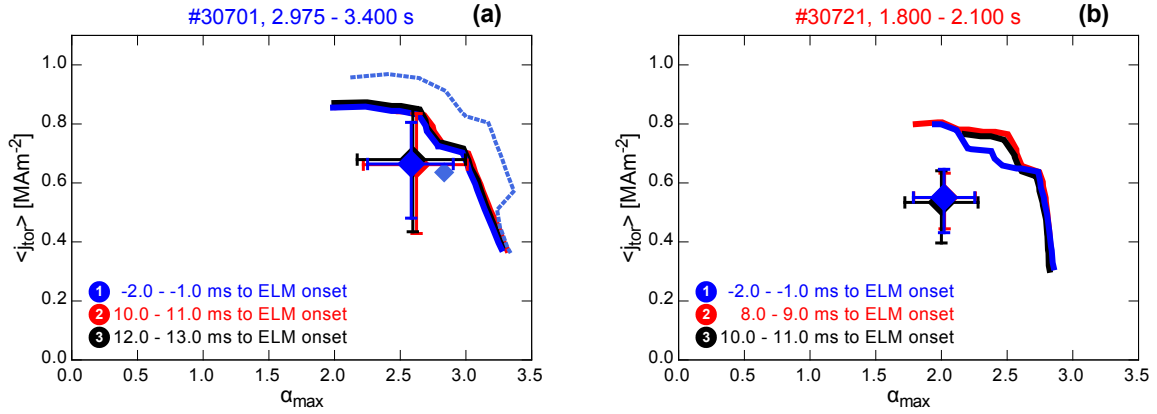


Figure 3:  $j$ - $\alpha$  diagrams for phases in which the high frequency fluctuations are present: (a) #30701, for comparison the light-blue dashed boundary is calculated from a CLISTE equilibrium [10], and (b) #30721. For the analysed time intervals, stability boundaries and operational points are similar.

For every discharge three phases, in which the high frequency magnetic fluctuations are present, are analysed. Figure 3 presents the  $j$ - $\alpha$  diagrams of the stability analyses. The operational points are characterised by the maximum normalised pressure gradient ( $\alpha_{\text{max}}$ ) and the average toroidal current density in the pedestal ( $\langle j_{\text{tor}} \rangle$ ). The uncertainties of the operational point are calculated from the statistical errors of the  $ff'$  and  $p'$  profiles from the equilibrium input.

Both discharges are close to the peeling-ballooning boundary in the analysed intervals, which is in line with the observation that the high frequency fluctuations clamp the edge gradients at a stable level. In both cases no difference between the three analysed phases can be seen within the uncertainties, neither changes of the stability boundary nor movement of the operational point. This indicates that during the presence of the high frequency fluctuations the MHD behaviour of the pedestal does not change.

In summary, the clamping of the pedestal pressure gradients has been found to correlate with the onset of high frequency magnetic fluctuations. The detected fluctuation frequency scales with the neoclassically estimated  $E \times B$  background velocity at the plasma edge. Toroidal mode numbers of approximately 11 can be determined and also a significant magnetic fluctuation amplitude is detected on the HFS. During the presence of the fluctuations linear MHD stability analyses show stable operational points close to the peeling-ballooning boundary which do not evolve in time.

## References

- |   |   |
|---|---|
| [1] P. B. Snyder, et al. PoP <b>9</b> , 5 (2002)    | [6] F. M. Laggner, et al. PPCF <b>58</b> , 6 (2016) |
| [2] A. Burckhart, et al. PPCF <b>52</b> , 10 (2010) | [7] F. Mink, et al. submitted to PPCF (2016)        |
| [3] A. Diallo, et al. PRL <b>112</b> , 11 (2014)    | [8] R. Fischer, et al. to be submitted (2016)       |
| [4] X. Gao, et al. NF <b>55</b> , 8 (2015)          | [9] M. G. Dunne, et al. submitted to PPCF (2016)    |
| [5] W. L. Zhong, et al. PPCF <b>58</b> , 6 (2016)   | [10] P.J. McCarthy, et al. POP <b>6</b> , 9 (1999). |

## Acknowledgement

This work has been carried out within the framework of the EUROfusion Consortium and has received funding from the Euratom research and training programme 2014-2018 under grant agreement No 633053. The views and opinions expressed herein do not necessarily reflect those of the European Commission.

F. M. Laggner is a fellow of the Friedrich Schiedel Foundation for Energy Technology.